

Franco Benetollo · Emanuela Grigiotti
Franco Laschi · Guido Pampaloni · Manuel Volpe
Piero Zanello

Electrochemical and EPR investigation on bis-toluene Cr(I) complexes. $[\text{Cr}(\eta^6\text{-CH}_3\text{C}_6\text{H}_5)_2][\text{dbcp-NO}_2]$ ($[\text{dbcp-NO}_2] = 1,2\text{-dibenzoyl-4-nitrocyclopentadienyl anion}$): the first example of a $[\text{Cr}(\eta^6\text{-CH}_3\text{C}_6\text{H}_5)_2]$ cation containing a *cis*-eclipsed arrangement of toluene rings

Received: 5 October 2004 / Revised: 22 February 2005 / Accepted: 4 March 2005 / Published online: 12 May 2005
© Springer-Verlag 2005

Abstract The reaction of $\text{Cr}(\eta^6\text{-CH}_3\text{C}_6\text{H}_5)_2$ with dbcpH-NO_2 ($\text{dbcpH-NO}_2 = 1\text{-benzoyl-3-nitro-6-hydroxy-6-phenyl fulvene}$) proceeds with the evolution of dihydrogen and formation of the ionic derivative $[\text{Cr}(\eta^6\text{-CH}_3\text{C}_6\text{H}_5)_2][\text{dbcp-NO}_2]$ ($\text{dbcp-NO}_2 = 1,2\text{-dibenzoyl-4-nitro-cyclopentadienyl anion}$) which was characterized by X-ray diffraction, electrochemical and EPR techniques. The cation $[\text{Cr}(\eta^6\text{-CH}_3\text{C}_6\text{H}_5)_2]^+$, which in the solid state presents an unprecedented *cis*-eclipsed arrangement of the arene rings, undergoes a chemically reversible, one-electron reduction to the corresponding neutral derivative.

Keywords Chromium(I) complexes · Substituted phenyl fulvene ligand · X-ray crystal structure · EPR spectroscopy · Electrochemistry

Introduction

One of the interesting features of cyclopentadiene is the fact that the proton acidity of the diene can vary to a broad span by varying the ring substituents [1], up to reaching the extreme case in which the proton is no longer on the ring system. If the substituents carry one or more oxygen atoms, it can be located on the

oxygen atoms themselves, thus actually transforming the cyclopentadiene in a fulvene derivative, see Structure 1.

On reaching the fulvene extreme of this equilibrium, the proton acidity will reach its maximum, as the proton itself is no more vincolated to any carbon atom. A search in the literature revealed that fulvene derivatives bearing an hydroxyl group in position 6 show a strong acidic behaviour due to intramolecular hydrogen bonding, as demonstrated by the chemical shift of the hydroxyl proton, always appearing in very low-field regions of the $^1\text{H-NMR}$ spectrum of solution of the compounds in apolar solvents (complete ionization is observed in polar solvents, see Structure 2) [2–4].

These ligands have the interesting peculiarity that, on losing the hydroxyl proton during the redox reaction, they can rearrange to aromatic π -systems with a cyclopentadienyl core, thus favouring even more the course of the reaction.

In continuation of our studies concerning the synthesis and the reactivity of transition metal η^6 -arene derivatives [5–10], we have studied the reaction of $\text{Cr}(\eta^6\text{-CH}_3\text{C}_6\text{H}_5)_2$ with 1-benzoyl-3-nitro-6-hydroxy-6-phenyl fulvene, dbcpH-NO_2 [3], and in this paper, we report a study concerning the preparation and the properties of the ionic derivative $[\text{Cr}(\eta^6\text{-CH}_3\text{C}_6\text{H}_5)_2][\text{dbcp-NO}_2]$ ($\text{dbcp-NO}_2 = 1,2\text{-dibenzoyl-4-nitro-cyclopentadienyl anion}$), the first example of a bis-toluene chromium cation containing a *cis*-eclipsed conformation of the η^6 -bonded aromatic rings.

F. Benetollo
ICIS-CNR, Corso Stati Uniti 4, 35127 Padova, Italy

E. Grigiotti · F. Laschi · P. Zanello (✉)
Dipartimento di Chimica, Università di Siena, Via Aldo Moro,
53100 Siena, Italy
E-mail: zanello@unisi.it

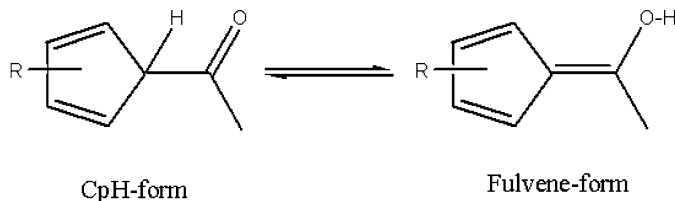
G. Pampaloni · M. Volpe
Dipartimento di Chimica e Chimica Industriale, Università di Pisa,
Via Risorgimento 35, 56126 Pisa, Italy
E-mail: pampa@dccl.unipi.it

Materials and methods

All manipulations of air and/or moisture-sensitive compounds were performed under an atmosphere of argon using standard Schlenk techniques. The reaction vessels were oven-dried at 150 °C prior to use, evacuated (10^{-2} mmHg) and then filled with nitrogen or argon.

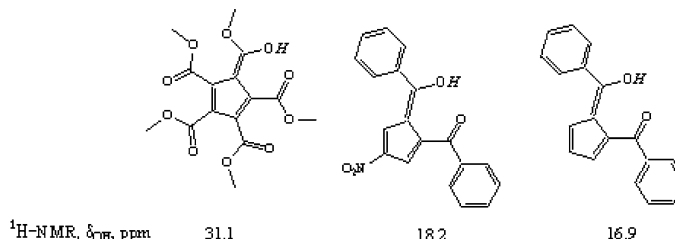
Structure 1 Equilibrium between the cyclopentadiene (CpH) and the fulvene forms of an oxygen-containing group substituted cyclopentadiene

Chart 1. Equilibrium between the cyclopentadiene (CpH) and the fulvene forms of an oxygen-containing group substituted cyclopentadiene.



Structure 2 Proton chemical shifts (CCl₄, RT) of the hydroxyl proton in 6-hydroxyl substituted fulvenes

Chart 2. Proton chemical shifts (CCl₄, RT) of the hydroxyl proton in 6-hydroxyl substituted fulvenes.



IR spectra were recorded with a Perkin Elmer mod. FT 1725X spectrophotometer on nujol mulls prepared under rigorous exclusion of air.

Chromium bis(toluene), Cr(η^6 -CH₃C₆H₅)₂ [5], and 1-benzoyl-3-nitro-6-hydroxy-6-phenyl fulvene [3] were prepared as reported in the literature.

Materials and apparatus for electrochemistry and joint EPR measurements were described elsewhere [11]. Potential values are referred to the saturated calomel electrode (SCE). Under the present experimental conditions, the one-electron oxidation of ferrocene occurs at $E^{\circ'} = +0.39$ V.

Preparation of [Cr(η^6 -CH₃C₆H₅)₂][dbcp-NO₂]

The compound Cr(η^6 -CH₃C₆H₅)₂ (0.404 g, 1.71 mmol) was added to a well-stirred suspension of an equimolar amount of 1-benzoyl-3-nitro-6-hydroxy-6-phenyl fulvene (0.540 g, 1.71 mmol) in THF (120 ml). The mixture turned immediately bloody red with abundant solid at the bottom of the flask. As soon as the gas evolution (H₂ by gas-chromatography) ceased, the suspension was filtered leaving an orange–yellow precipitate, which was washed with THF (5 ml) and vacuum-dried. The compound [Cr(η^6 -CH₃C₆H₅)₂][dbcp-NO₂] (0.619 g, 66% yield) was recovered as a bright yellow powder. A sample of this solid was suspended in THF, refluxed for 20 min and then filtered while hot; by slow cooling, crystals of the compound, as thin yellow rectangular slabs, were obtained. Anal. found (calc.) for C₃₃H₂₈CrNO₄: C 69.1% (70.5), H 4.7% (5.0), N 2.5% (2.5). IR (nujol, cm⁻¹): 3,058 w, 1626 m, 1,606 s, 1,574 s, 1,495 w, 1,400 s, 1,357 m, 1,250 s, 1,212 s, 1,150 m, 1,074 m, 942 m, 867 m, 840 m, 814 m, 781 m, 758 m, 725 s, 706 m.

X-Ray Structure Determination for [Cr(η^6 -CH₃C₆H₅)₂][dbcp-NO₂]

Crystal data and structure refinement are given in Table 1. A prismatic red–orange crystal was lodged in Lindemann glass capillary and sealed in nitrogen atmosphere and centred on a four-circle Philips

PW1100 diffractometer operating in $\theta/2\theta$ scan mode with graphite-monochromated MoK α radiation, following standard procedures at room temperature. The intensity data were corrected for Lorentz-Polarization effects and for absorption, as described by North et al.

Table 1 Crystal data and structure refinement

Compound	[Cr(η^6 -CH ₃ C ₆ H ₅) ₂][dbcp-NO ₂]
Empirical formula	C ₃₃ H ₂₈ CrNO ₄
Formula weight	554.56
Temperature (K)	293(2)
Wavelength (Å)	0.71073
Crystal system	monoclinic
Space group	<i>P</i> 2 ₁ / <i>a</i>
Unit cell dimensions	<i>a</i> = 11.470(3) Å <i>b</i> = 20.370(4) Å <i>c</i> = 11.886(3) Å β = 103.57(3)°
Volume (Å ³)	2700(1)
<i>Z</i>	4
<i>D</i> _c (Mg/m ³)	1.364
μ (mm ⁻¹)	0.463
<i>F</i> (000)	1156
θ range for data collection	3–22°
Index ranges	–12 ≤ <i>h</i> ≤ 11, 0 ≤ <i>k</i> ≤ 21, 0 ≤ <i>l</i> ≤ 12
Reflections collected	2,658
Independent reflections	2,533 [<i>R</i> _{int} = 0.0255]
Data/restraints/parameters	2533/0/356
Goodness-of-fit on <i>F</i> ²	1.316
Final <i>R</i> indices [<i>I</i> ≥ 2 σ (<i>I</i>)]	<i>R</i> ₁ = 0.097; <i>w R</i> ₂ = 0.195

Fig. 1 ORTEP diagram of $[\text{Cr}(\eta^6\text{-CH}_3\text{C}_6\text{H}_5)][\text{dbcp-NO}_2]$. Thermal ellipsoids are drawn at 30% probability level

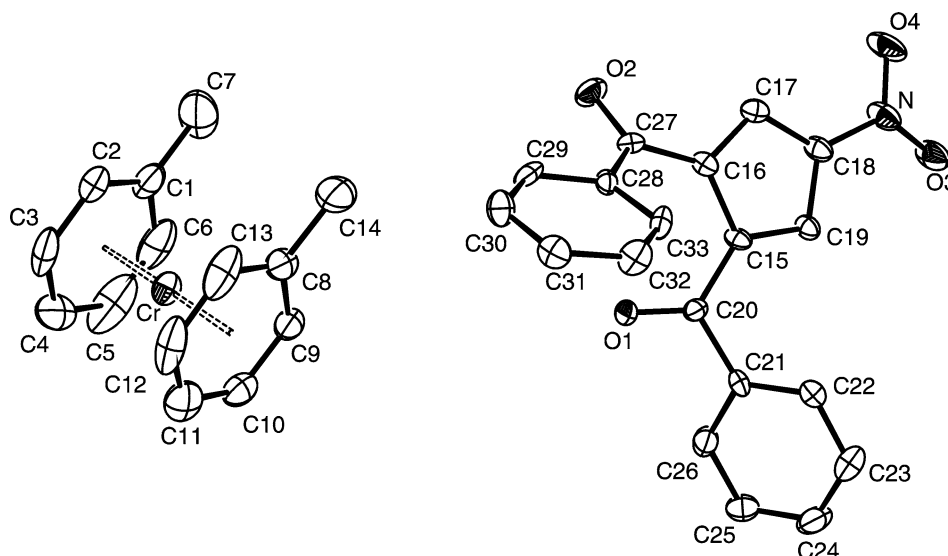


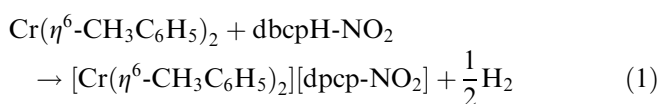
Table 2 Selected bond lengths (Å) and angles (°) for $[\text{Cr}(\eta^6\text{-CH}_3\text{C}_6\text{H}_5)_2][\text{dbcp-NO}_2]$

Cr–C(5)	2.09(2)	Cr–C(11)	2.10(1)
Cr–C(4)	2.10(1)	Cr–C(12)	2.11(1)
Cr–C(10)	2.12(1)	Cr–C(13)	2.12(1)
Cr–C(3)	2.13(1)	Cr–C(6)	2.14(1)
Cr–C(2)	2.19(1)	Cr–C(9)	2.15(1)
Cr–C(8)	2.16(1)	Cr–C(1)	2.18(1)
O(1)–C(20)	1.23(1)	O(2)–C(27)	1.24(1)
O(3)–N	1.21(1)	O(4)–N	1.25(1)
N–C(18)	1.42(1)	C(15)–C(19)	1.39(1)
C(15)–C(16)	1.45(1)	C(15)–C(20)	1.45(1)
C(16)–C(17)	1.36(1)	C(16)–C(27)	1.47(1)
C(17)–C(18)	1.40(1)	C(18)–C(19)	1.40(1)
C(20)–C(21)	1.49(1)		
O(3)–N–O(4)	123.5(9)	O(3)–N–C(18)	120.5(9)
O(4)–N–C(18)	116.1(9)	C(19)–C(18)–C(17)	109.4(8)
C(19)–C(18)–N	123.6(9)	C(17)–C(18)–N	126.9(9)
O(1)–C(20)–C(15)	122.3(8)	O(1)–C(20)–C(21)	118.8(8)
O(2)–C(27)–C(16)	120.3(8)	O(2)–C(27)–C(28)	119.9(8)

[12]. The structure was solved by standard direct methods (SIR 97) [13]. Refinement was carried out by full-matrix least-squares techniques on F^2 . All non-hydrogen atoms were refined with anisotropic thermal parameters. The H-atoms were placed in calculated at idealized positions using a riding model with fixed isotropic thermal parameters ($1.2 U_{\text{equiv}}$ of the parent carbon atom). Structure refinement and final geometrical calculations were carried out with SHELXL-97 program [14], implemented in the WinGX package [15].

Results and discussion

The reaction of dbcpH-NO_2 with $\text{Cr}(\eta^6\text{-CH}_3\text{C}_6\text{H}_5)_2$ is fast as formation of a yellow solid occurs within minutes from mixing of the reagents, see eq. 1.

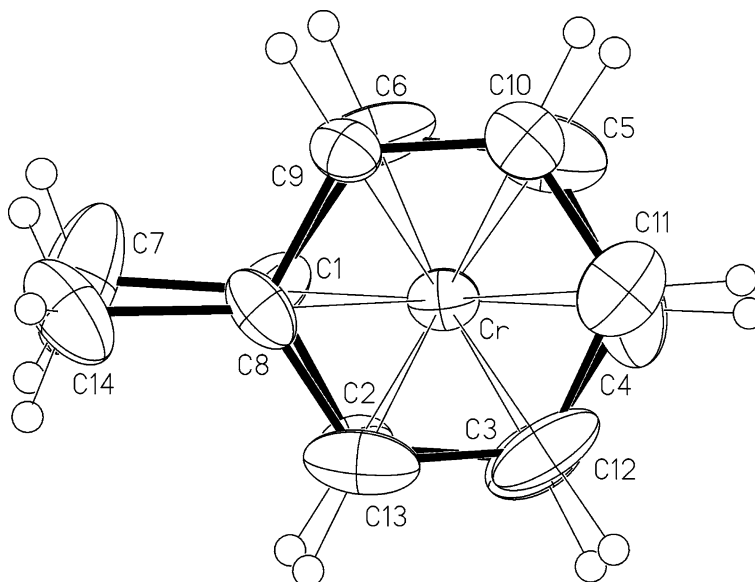


After many attempts, recrystallization from boiling THF affords crystals suitable for an X-ray investigation. Although the low quality of crystals did not allow a high quality structural study, some interesting evidences have been collected. The structure consists of separated $[\text{Cr}(\eta^6\text{-CH}_3\text{C}_6\text{H}_5)_2]^+$ cations and $[\text{dbcp-NO}_2]^-$ anions. An ORTEP plot of the molecular structure is shown in Fig. 1, while selected bond lengths and angles are in Table 2.

The C–C distances within the arene rings of the cation [$1.38(2)$ Å, av.], the perpendicular distances [$1.61(1)$ Å, av.] from the Cr atom to the arene planes, the angle between the arene ligands [$175.4(5)^\circ$] and the distances Cr–C(arene) are in the range observed in other bis(η^6 -toluene) chromium(I) derivatives [16–23]. The striking feature of this derivative is the conformation of the arene rings in the cationic moiety that represent the first example of almost *cis*-eclipsed conformation of the toluene ligands, see Fig. 2, whereas all of the $[\text{Cr}(\eta^6\text{-CH}_3\text{C}_6\text{H}_5)_2]^+$ cations known to date adopt invariably a *trans*-eclipsed conformation of the arenes [16–23].

The anion reported in this paper represents a novel species, only the synthesis of the protonated derivative and its molecular structure being reported in the literature [3]. The five-membered ring of the anion shows C–C bond distances and angles similar to those observed in the protonated species and are comprised between $1.36(1)$ and $1.40(1)$ Å, except for C(15)–C(16) distance which is to $1.45(1)$ Å in the anion and $1.467(2)$ Å in the fulvene [3]. The nitro group is substantially coplanar with the cyclopentadienyl ring; the dihedral angle being 1.5° in the protonated species and 2.4° in our compound. The C(18)–N bond distance of

Fig. 2 View of the $[\text{Cr}(\eta^6\text{-CH}_3\text{C}_6\text{H}_5)_2]^+$ cation in $[\text{Cr}(\eta^6\text{-CH}_3\text{C}_6\text{H}_5)[\text{dbcp-NO}_2]]$ along the toluene-Cr-toluene axis



1.42(1) Å is similar to that observed in dbcpH-NO_2 [1.433(4) Å] [3].

Although the large standard deviations, a significant difference between the protonated and the deprotonated species is observed for the C=O and the $\text{C}_{\text{carbonyl}}\text{-C}_{\text{five-membered ring}}$ bond distances whose averaged values amount to 1.22(1) and 1.46(1) Å, the corresponding distances in dbcpH-NO_2 being 1.279(4) and 1.425(4) Å [3]. Short C–O and long C–C distances are observed in 1,2-aroyl substituted aromatics such as 1,2-dimesitylbenzene [C=O: 1.214, 1.213 Å; $\text{C}_{\text{aromatic}}\text{-C}_{\text{carbonyl}}$: 1.502, 1.501 Å] [24] and 4,5,12,13-tetrabenzoyl[2,2]paracyclophane [C=O: 1.218(3) av. Å; $\text{C}_{\text{aromatic}}\text{-C}_{\text{carbonyl}}$: 1.500(3) av. Å] [25]. The shorter C–O distances and the longer C–C ones suggest that the electron delocalization typical of dbcpH-NO_2 , which involves the five-membered ring and the proton located in between the two carbonyl oxygen atoms, is lost and that the electron delocalization of the resulting species is limited to the five-membered ring which can be thus considered a cyclopentadienyl anion.

Figure 3 shows the X-band EPR spectra of $[\text{Cr}(\eta^6\text{-CH}_3\text{C}_6\text{H}_5)_2][\text{dbcp-NO}_2]$ in CH_3CN solution, under different experimental conditions. The pertinent experimental parameters are collected in Table 3.

The temperature-dependent line shape analysis is suitably performed accounting for the $S=1/2$ Spin Electron Hamiltonian (isotropic in fluid solution, rhombic both in glassy solution and in the solid state) with noticeable resolution of hyperfine (hpf) splittings in fluid solution.

The glassy spectrum, Fig. 3a, is characterized by three signals with significant resolution for the low- and medium-field spectral regions, whereas the high-field region is broad and totally unresolved.

Even if the g_i and a_i parameters are typical of a doublet paramagnetic species, in which the electron is

mainly delocalized on the aromatic ligands, a significant metallic character is undoubtedly present ($g_i \neq g_{\text{electron}}=2.0023$; reduced $\Delta H_{\text{isotropic}}$). The direct magnetic interaction of the unpaired electron with the “5 + 5” ^1H nuclei of the two aromatic rings should afford eleven hpf signals (relative intensities ratio: 1:10:45:120:210:252:210:120:45:10:1) in the three anisotropic spectral regions.

As a matter of fact, the intermediate-field absorption (g_m) exhibits nine hpf lines, probably because of both the different line widths (ΔH_i), and the eventual line broadening effects played by the coordinating ability of the solvent (CH_3CN).

It looks credible that the overall anisotropic features (i.e. spectral rhombicity, different g_i regions broadening, partial hpf resolution) might arise from some distortions in the primary coordinating geometry triggered by the steric effects of the peripheral methyl groups.

No ^{53}Cr isotopic satellite peaks are detectable ($^{53}\text{Cr}:\text{I}=3/2$, natural abundance = 9.55%).

As shown in Fig. 3b–c, at the glassy-solution transition ($T=229$ K), the anisotropic features collapse in broad and poorly resolved isotropic absorptions, which in the second derivative display resolution of only seven hpf lines.

Because of the presence of reduced structural anisotropy under fast motion condition [26, 27], the fluid solution exhibits limited $m_I(^1\text{H})$ dependence of the paramagnetic splittings. Tentatively, this could arise from different paramagnetic interactions of the *ortho-para* vs. the *meta* ^1H nuclei, even if it cannot be ruled out that the relatively limited spectral resolution might mask a higher number of ^1H signals. The isotropic spectrum exhibits two broad ^{53}Cr isotopic satellite wings again testifying to the small, but detectable, metallic character.

The average glassy features well fit those at room temperature, thus confirming the basic maintenance of

Table 3 X-band EPR experimental parameters of the cation $[\text{Cr}(\eta^6\text{-CH}_3\text{C}_6\text{H}_5)_2]^+$ in $[\text{Cr}(\eta^6\text{-CH}_3\text{C}_6\text{H}_5)_2][\text{dbcp-NO}_2]$ under different experimental conditions

Physical state	g_1^a	g_m^a	g_h^a	δg^a	$\langle g \rangle^a$	g_{iso}^a	$a_1^{b,c}$	$a_m^{b,c}$	$a_h^{b,c}$	$\langle a \rangle^{b,c}$	$a_{\text{iso}}^{b,c}$	ΔH_{iso}^b
MeCN solution	2.006	1.988	1.959	0.047	1.984	1.988	3	4	$\leq 20/6$	≤ 3	4	13
Solid state	2.001 ^d	1.984 ^d	1.968 ^d	0.033 ^d	1.984 ^d		$\leq 15^f$	$\leq 13^g$	$\leq 13^h$	$\leq 13^i$		
	2.002 ^e	1.984 ^e	1.969 ^e	0.033 ^e	1.985 ^e		$\leq 13^f$	$\leq 12^g$	$\leq 10^h$	$\leq 12^i$		

$$\langle g \rangle = 1/[3(g_1 + g_m + g_h)], \langle a \rangle = 1/[3(a_1 + a_m + a_h)], \langle \Delta H \rangle = 1/[3(\Delta H_1 + \Delta H_m + \Delta H_h)]$$

^a g_i : ± 0.005

^b $a_{\text{isotropic}}, a_{\text{anisotropic}}$ in Gauss

^c $a_{\text{anisotropic}}$: ± 3 G, $a_{\text{isotropic}}$: ± 1 G

^d $T = 105$ K

^e $T = 298$ K

^fExperimental ΔH_1

^gExperimental ΔH_m

^hExperimental ΔH_i ; Experimental $\langle \Delta H \rangle$

the primary geometry under different experimental conditions.

In the solid state, at room temperature, $[\text{Cr}(\eta^6\text{-CH}_3\text{C}_6\text{H}_5)_2]^+$ exhibits a broad axial lineshape (first derivative). The absence of any hpf resolution as well as of the ^{53}Cr satellite signals is due to the active spin-spin paramagnetic interactions which accelerates the Electron Spin relaxation mechanisms [26]. At low temperature, the spectrum exhibits a lineshape quite similar to that detected at room temperature, even if the actual line-width is significantly broader as a consequence of more effective Electron Spin relaxation mechanisms. This further supports that, in very different experimental conditions and aggregation states, the main geometry of the Cr(I) complex is basically retained.

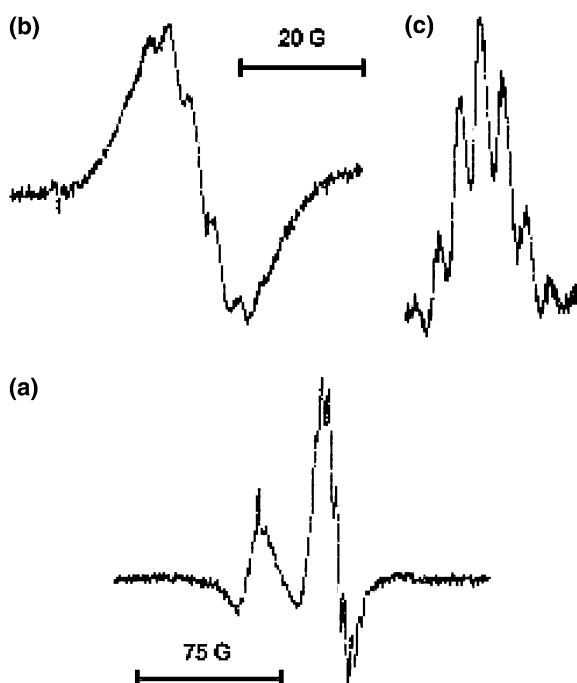


Fig. 3 X-Band EPR spectra recorded in MeCN solution of $[\text{Cr}(\eta^6\text{-CH}_3\text{C}_6\text{H}_5)_2]^+$ in $[\text{Cr}(\eta^6\text{-CH}_3\text{C}_6\text{H}_5)_2][\text{dbcp-NO}_2]$. **a** Second derivative spectrum under glassy condition ($T = 105$ K), **b** first and **c** second derivative profiles in fluid solution ($T = 298$ K)

Figure 4 shows the cathodic cyclic voltammetric behaviour of the monocation $[\text{Cr}(\eta^6\text{-CH}_3\text{C}_6\text{H}_5)_2]^+$ from $[\text{Cr}(\eta^6\text{-CH}_3\text{C}_6\text{H}_5)_2][\text{dbcp-NO}_2]$ in deaerated MeCN solution.

It undergoes a reduction process exhibiting features of chemical reversibility in the cyclic voltammetric time scale ($E^{\circ'} = -0.90$ V; $\Delta E_p = 68$ mV at 0.1 Vs $^{-1}$). Controlled potential coulometry failed in determining the number of electrons involved in such cathodic step, in that relatively fast reoxidation triggered by traces of air continually tended to regenerate the original monocation. Nevertheless, periodical control by cyclic voltammetry on the partially reduced solution afforded responses similar to the original ones, thus confirming that no decomposition of the original framework takes place upon reduction.

Just to prove that, as happens for related Cr(I) complexes [10], the reduction process involves a one electron per molecule, an equimolar amount of 1,1'-ferrocenedimethanol was added as an internal standard. As a matter of fact, such ferrocendiyl derivative, which undergoes a one-electron oxidation at $E^{\circ'} = +0.37$ V, possesses a molecular weight similar to that of the Cr(I)

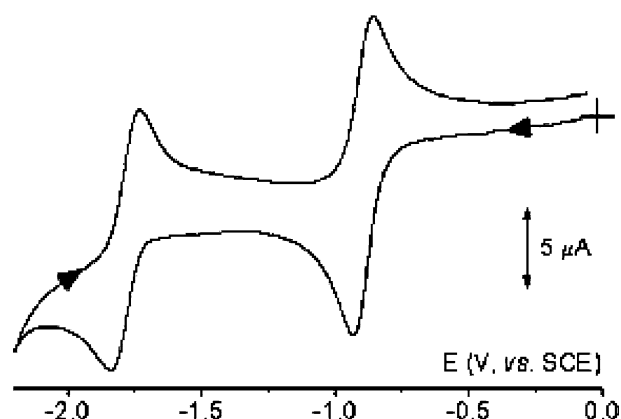


Fig. 4 Cyclic voltammogram recorded at a gold electrode in a MeCN solution containing $[\text{Cr}(\eta^6\text{-CH}_3\text{C}_6\text{H}_5)_2][\text{dbcp-NO}_2]$ (1.2×10^{-3} M). $[\text{NBu}_4][\text{PF}_6]$ (0.2 M) supporting electrolyte. Scan rate 0.2 Vs $^{-1}$

monocation (246 vs. 236), thus implying comparable diffusion coefficients [11].

Analysis of the reduction process with scan rate progressively varying from 0.02 Vs^{-1} to 2 Vs^{-1} confirms the occurrence of a simple one-electron process, coupled to weak adsorption of the reagent at the electrode surface. In fact, the current function $i_{pc} \cdot v^{-1/2}$ tends to increase with the scan rate, whereas the current ratio i_{pa}/i_{pc} , which is 1 at low scan rate, tends to decrease with the scan rate [11].

The electrochemical reversibility of the Cr(I)/Cr(0) passage, as testified by a peak-to-peak separation constantly close to the theoretical value of 59 mV, suggests that the reduced neutral complex maintains substantially the structural geometry of the monocation precursor.

As shown in Fig. 4, $[\text{Cr}(\eta^6\text{-CH}_3\text{C}_6\text{H}_5)_2][\text{dbcp-NO}_2]$ exhibits a further reversible reduction ($E^{o'} = -1.79 \text{ V}$), which is assigned to the $\text{NO}_2/\text{NO}_2^-$ process from the counteranion.

Even if not shown in the figure, an irreversible oxidation is also present ($E_p = +0.89 \text{ V}$) in the cyclic voltammogram, which is tentatively assigned to the oxidation of the Cr(I) monocation to a quite unstable Cr(II) dication (no return peak was detected even at scan rates of $10\text{--}20 \text{ Vs}^{-1}$).

Acknowledgments Thanks are due to the Ministero dell'Istruzione dell'Università e della Ricerca (MIUR, Roma), Programma di Ricerca Scientifica di Notevole Interesse Nazionale 2002–2003 for financial support and to Professor Fausto Calderazzo for helpful discussions. Piero Zanello acknowledges the financial support of the University of Siena (PAR 2003).

References

- Bordwell FG, Cheng J, Bausch MJ (1988) *J Am Chem Soc* 110:2872
- Linn WJ, Sharkey WH (1957) *J Am Chem Soc* 79:4970
- Ferguson G, Marsh WC, Restivo RJ, Lloyd D (1975) *J Chem Soc Perkin Trans II* 998
- Bruce MI, Walton JK, Skelton BW, White AH (1982) *J Chem Soc Dalton Trans* 2209
- Calderazzo F, Invernizzi R, Marchetti F, Masi F, Moalli A, Pampaloni G, Rocchi L (1993) *Gazz Chim Ital* 123:53
- Calderazzo F, Pampaloni G (1995) *J Organomet Chem* 500:47
- Calderazzo F, De Benedetto GE, Englert U, Ferri I, Pampaloni G, Wagner T (1996) *Z Naturforsch* 51b:506
- Calderazzo F, De Benedetto, GE Detti, S Pampaloni G (1997) *J Chem Soc Dalton Trans* 3319
- Calderazzo F, Ferri I, Pampaloni G, Green MLH (1998) *Organometallics* 16:3100
- Schneider JJ, Czap N, Spickermann D, Lehmann CW, Fontani M, Laschi F, Zanello P (1999) *J Organomet Chem* 590:7
- Zanello P (2003) *Inorganic electrochemistry. Theory, practice and application*. RSC, Oxford
- North ATC, Phillips DC, Mathews FS (1968) *Acta Crystallogr* A24:351
- Altomare A, Burla MC, Cavalli M, Cascarano GL, Giacovazzo C, Gagliardi A, Moliterni AGG, Polidori G, Spagna R (1999) "SIR-97" *J Appl Crystallogr* 32:115
- Sheldrick GM (1997) SHELXL-97, Program for the refinement of crystal structures, University of Göttingen
- Farrugia LJ (1999) *J Appl Crystallogr* 32:837
- Starovskii OV, Struchkov YuT (1961) *Zh Strukt Khim* 2:162
- Shibaeva RP, Atovmyan LO, Rozenberg LP (1969) *J Chem Soc Chem Commun* 649
- Shibaeva RP, Atovmyan LO, Orfanova MN (1969) *J Chem Soc Chem Commun* 1494
- Broderick WE, Kwang WC, Wai CW (1997) *Proc Electrochem Soc* 97:1102
- Braga D, Costa AL, Grepioni F, Scaccianoce L, Tagliavini E (1997) *Organometallics* 16:2070
- Grepioni F, Cojazzi G, Draper SM, Scully N, Braga D (1998) *Organometallics* 17:296
- Braga D, Draper SM, Champeil E, Grepioni F (1999) *J Organomet Chem* 573:73
- Honnorscheid A, Dinnebiec RE, Jansen M (2002) *Acta Crystallogr B* 58:482
- Bock H, Nick S, Naether C, Bensch WZ (1995) *Naturforsch* 50b:605
- Koenig B, Ramm S, Bubenitschek P, Jones PG, Hopf H, Knieriem B, de Meijere A (1994) *Chem Ber* 127:2263
- Mabbs FE, Collison D (1992) *Electron paramagnetic resonance of d transition metal compounds*. In: *Studies in inorganic chemistry*, vol 16. Elsevier, New York
- Drago RS (1992) *Physical methods for chemists*. Saunders College Publ, New York